Radiomics-based method for diagnosis of calciphylaxis in patients with chronic kidney disease using computed tomography

Qian Yu[1], Yuqiu Liu[2], Xiaotong Xie[2], Jinqiang Liu[1], Shan Huang[1], Xiaoliang Zhang[2], Shenghong Ju[1]

[1]Department of Radiology, Jiangsu Key Laboratory of Molecular and Functional Imaging, Zhongda Hospital, Medical School, Southeast University, Nanjing, China; [2]Institute of Nephrology, Zhongda Hospital, Medical School, Southeast University, Nanjing, China

Contributions: (I) Conception and design: S Ju, X Zhang; (II) Administrative support: S Ju, X Zhang; (III) Provision of study materials or patients: Q Yu, Y Liu, S Huang; (IV) Collection and assembly of data: Q Yu, X Xie, J Liu, S Huang; (V) Data analysis and interpretation: Q Yu; (VI) Manuscript writing: All authors; (VII) Final approval of manuscript: All authors.

Correspondence to: Shenghong Ju, MD, PhD. Professor of Medicine, Department of Radiology, Jiangsu Key Laboratory of Molecular and Functional Imaging, Zhongda Hospital, Medical School, Southeast University, 87 Ding Jia Qiao Road, Nanjing, China. Email: jsh0836@hotmail.com.

Abstract: Calciphylaxis is a rare, life-threatening condition that affects patients with chronic kidney disease (CKD) undergoing dialysis. Skin biopsy as the gold standard causes ulceration, bleeding, or infection. This study aimed to develop radiomic methods using CT as a noninvasive method for calciphylaxis diagnosis. The confirmed calciphylaxis patients (Group I), pathologically confirmed non-calciphylaxis patients (Group II), and CKD patients (Group III) from October 1, 2017, to November 30, 2019, were enrolled. Training: 70% of patients of Group I and all Group III. Test: 30% of patients of Group I and all Group II. ROI was set at the skin lesion including the soft tissue. First-order and texture features were extracted from each lesion unit. CT-based radiomic models were on the basis of logistic regression (LR) and support vector machine (SVM). Additionally, model performance was evaluated in the test dataset and compared with the plain radiography and bone scintigraphy. In total, 124 lesions and 38 lesions were identified in training and test datasets. Radiomic models were effective in detecting calciphylaxis in patients with CKD, with AUCs of 0.93 (95% CI: 0.924–0.953) and 0.93 (95% CI: 0.921–0.953) (SVM and LR) in test. The SVM model manifested a sensitivity and specificity of 0.89 and 0.8, and 0.78 and 0.90, at high-sensitivity and high-specificity operating points, respectively. Similar performance was found in the LR model. Radiomic models were more effective than plain radiography and bone scintigraphy (Delong test, P<0.05). Verification studies showed the features which manifested the real variability of lesions. In this research, it primarily developed a radiomic method for noninvasive detection of calciphylaxis in patients with CKD. Through this method, calciphylaxis can be detected when invasive procedures are not feasible.

Keywords: Calciphylaxis; computed tomography (CT); radiomics

Introduction

Calciphylaxis is a rare, life-threatening condition with high morbidity and mortality, commonly affecting patients with chronic kidney disease (CKD) undergoing dialysis, with death caused mainly by sepsis secondary to infected ulcers (1).

Calciphylaxis diagnosis is challenging, for which skin biopsy is a gold standard. Nonetheless, it increases the risk of ulceration, bleeding, and necrosis owing to deep incisions (2). A noninvasive tool for diagnosing calciphylaxis lesions is beneficial for patients with skin lesions and CKD.

The potential usefulness of noninvasive radiology,

including plain radiography and bone scintigraphy, has been reported, whereas the usefulness of computed tomography (CT) has not been assessed (3-5). We hypothesized that histological changes, covering vessel calcification, thrombosis, interstitial calcium deposits, and adipose tissue remodelling, in the subcutaneous tissue of calciphylaxis lesions (1,2,6-8) would be reflected in the CT value and texture adopting the radiomic method, which is a high-throughput approach using image features calculated from histogram and texture analysis (9,10).

Hence, this research aims to develop and test a CT-based radiomic model for noninvasive detection of calciphylaxis in patients with CKD.

Methods

Study population

This retrospective, cohort study was conducted in accordance with the Declaration of Helsinki (as revised in 2013) and was approved by the local institutional ethics review board. Additionally, the need for written informed consent from the participants was waived.

In this research, it retrospectively reviewed the institutional datasets for patients with the initial diagnosis of calciphylaxis from October 1, 2017, to November 30, 2019. Calciphylaxis diagnosis protocol was based on "Criteria for Diagnosis of Calciphylaxis" illustrated by McCarthy *et al.* (11) One patient with risk factors and clinical conditions would undergo histopathological examination and receive multidisciplinary discussion involving nephrology, dermatology, radiology, and pathology departments with experienced doctors (12,13). If one is finally diagnosed with calciphylaxis as revealed in the histopathological result, he or she was included as calciphylaxis patients (Group I). If one with possible calciphylaxis but finally ruled out by histopathology, he or she was considered as suspected calciphylaxis patients (pathologically confirmed non-calciphylaxis patients) (Group II). Viscera calciphylaxis was not included in the analysis.

In the next step, CT scan data involving lesion location was searched. For instance, if one patient had ulceration in the right leg, the researcher would find lower extremities' non-contrast CT images in Picture Archiving and Communication Systems. All CT scan followed routine CT scan protocols.

Nevertheless, for limited negative cases, based on the hypothesis, Patients with CKD underwent dialysis during the same time period with abdominal CT, who displayed no features of calciphylaxis comprised the non-calciphylaxis cohort (CKD-non-calciphylaxis) (Group III), so as to extract radiomics features about subcutaneous tissue.

The training cohort comprised 70% of patients randomly selected from those with calciphylaxis and all non-calciphylaxis patients with CKD.

The independent test cohort consisted of the remaining 30% of patients with calciphylaxis and all patients suspected of having calciphylaxis. There was no overlapping between training and test data.

Radiomic analysis and model building

Figure 1 displays the pipeline of the radiomic model with the feature extraction and model building on each lesion unit.

Lesion segmentation

The CT images containing the lesion patches were segmented using 3Dslicer (version 4.10.0; https://www.slicer.org/) (*Figure 1*). As determined by an experienced nephrologist and radiologist based on photos or records, a 50×50×50 mm³ box was placed in the area of the lesion for patients with calciphylaxis and those suspected of calciphylaxis. For CKD-non-calciphylaxis patients, 2 boxes of the same size were placed at the L3 vertebra of their backs. Apart from muscle and bone in the box, all subcutaneous tissues would be segmented as lesion patches.

Feature extraction

In the first step, all images and masks were resampled to form isotropic voxels of unit dimension with 1 voxel corresponding to 1 mm³ to guarantee comparability. By centring the image at the mean with a standard deviation and re-charting the histogram to conform to l±3r (l: the average grey level within the VOI; r: the grey-level standard deviation), image normalization was realised.

For each lesion, there were a total of 774 features. In accordance with pyradiomics, both first-order and textural features were calculated from the original images and those with the wavelet filter (14).

Model building

Normalisation was applied to the feature matrix with each vector featured with a zero centre and standard deviation.

To reduce the space dimensionality of the feature, the Pearson correlation coefficient (PCC) of the feature pair
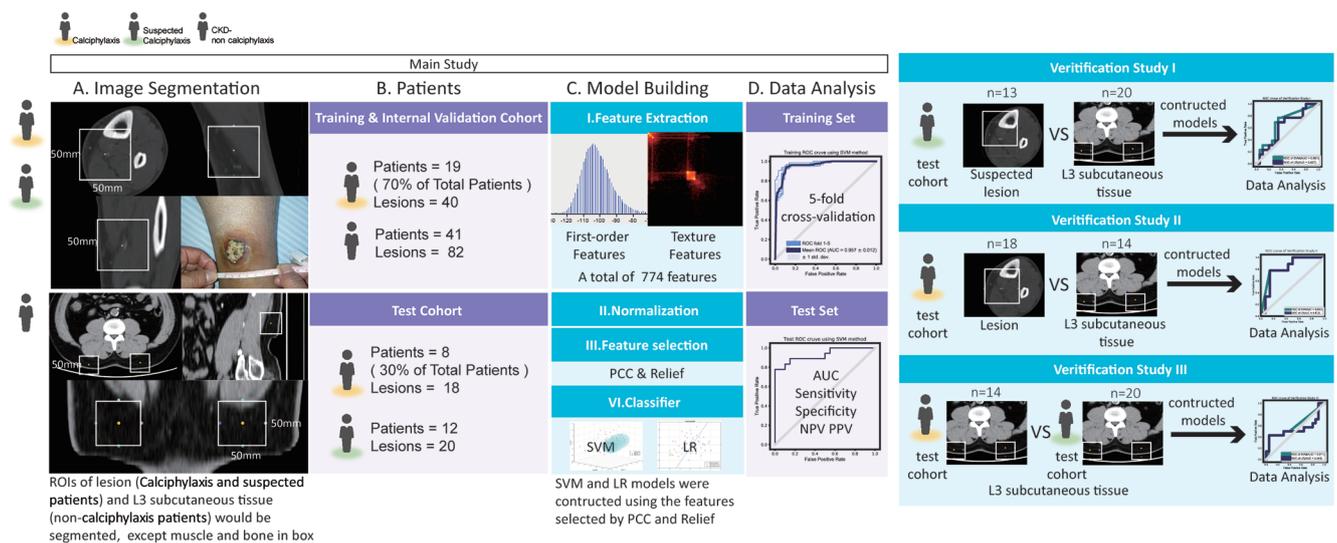
Figure 1 Flow chart of main study and verification studies. AUC, areas under the ROC curves; CKD, chronic kidney disease; LR, logistic regression; SVM, support vector machine; ROI, region of interest; PPV, positive predictive value; NPV, negative predictive value; ROC, receiver operating characteristic; PCC, Pearson correlation coefficient.

was adopted. Subsequently, Relief was employed to identify the features most closely correlated with the outcome, selecting the sub dataset and finding relative features according to the label by recursion.

The model and the robustness of the extracted features were built and verified, respectively, through two different supervised learning algorithms, namely the support vector machine (SVM) and the logistic regression (LR) (15). The former searches the hyper-plane to label the cases by mapping the features in a higher dimension, whereas the latter is deemed as a linear classifier via penalised maximum likelihood. Moreover, the linear kernel was used for explicable feature coefficients in the SVM model. In the training course, the 5-fold cross-validation of the training dataset was conducted to confirm the model's performance.

Model performance and stability

High specificity and sensitivity points
In line with the method described in Chilamkurthy *et al.* (16), high specificity and sensitivity points were selected from the receiver operating characteristic (ROC) curve of the training dataset.

Model performance
The test dataset was adopted for the performance evaluation of the model. More specifically, areas under the ROC

curves (AUCs), as well as the sensitivity, specificity, negative predictive value (NPV), and positive predictive value (PPV), at these 2 operating points were recorded.

Since the diagnostic performance of plain radiography (presence of vascular calcification in lesion peripheries) and bone scintigraphy in the test dataset was assessed, the AUCs of the radiomic model were compared with those of other radiological methods through the Delong test.

Verification studies
To determine the ability of the model to identify the calciphylaxis lesion in CKD patients, rather than classify the extremities and abdomen tissue: (I) this research did not extract shape-based features and designed three verification studies. (II) prior to study, it researched the abdomen CT scan at the time of initial diagnosis in the test dataset.

For calciphylaxis patients, 7 patients had abdomen CT scan without skin lesions at back or abdomen, and a total of 14 patches segmented manifested in *Figure 1*. For suspected calciphylaxis patients, 7 of 12 patients (13 of 20 lesions) were not at the back or abdomen, and they had an abdomen CT scan at the time of initial diagnosis. Another three suspected patients with abdomen CT scan were covered as well. Consequently, a total of 20 (7×2+3×2) abdomen subcutaneous patches were segmented in suspected calciphylaxis patients (*Figure 1*).

Study I: there was a comparison between the results

of the suspected lesion and L3 subcutaneous tissue in suspected calciphylaxis patients.

Study II: there was a comparison between skin lesion and L3 subcutaneous tissue in calciphylaxis patients. Patients with skin lesion in the back would be excluded.

Study III: there was a comparison between L3 subcutaneous tissue in calciphylaxis patients and suspected calciphylaxis patients.

Statistical analysis

In order to assess the patients' clinical and demographic characteristics, the Chi-square test (or the Fisher's exact test if necessary) was conducted to assess categorical variables, while the Mann-Whitney test was used for evaluating continuous variables in SPSS (version 22.0. IBM Crop. Armonk, NY, USA). Then, feature selection and model establishment were realised through FeAture Explorer (FAE, v0.2.5, https://github.com/salan668/FAE) on Python (3.6.8, https://www.python.org/). Furthermore, SPSS and Python were employed to calculate test values including the AUCs with 95% confidence interval (CI), the sensitivity, and the specificity. The Delong test was performed using the "pROC" package (R language 3.0.2, R Core Team, 2013), and a statistically significant P value should be smaller than 0.05.

Results

Patient characteristics

In this retrospective study, 32 patients diagnosed with calciphylaxis were enrolled in line with the histopathological result in Group I, and 15 patients suspected of having calciphylaxis in Group II, and finally, 27 and 12 patients with non-contrast CT scans containing skin lesions were enrolled in radiomics analysis respectively. Moreover, non-contrast CT scans containing skin lesions were included. Nevertheless, for limited negative cases, as shown in the hypothesis, 41 patients with CKD, undergoing dialysis during the same time period with abdominal CT, were enrolled in the non-calciphylaxis cohort (CKD-non-calciphylaxis) (Group III).

The training cohort comprised 70% (19/27) of patients with 40 lesions randomly selected from Group I and Group III (41 patients with 82 image patches). The independent test cohort comprised the rest 30% (8/27) of patients with calciphylaxis and Group II (12 patients with 20 lesions). Details about additional sample size consideration are

presented in the Appendix 1.

Baseline demographic and clinical characteristics of patients are outlined in *Table 1*. No dramatic differences existed in all baseline characters (P>0.05). The location of the skin lesions and CT scan of patients in Group I and II are listed in *Table 2*.

Performance of the radiomic model

The model, based on 8 features including 4 first-order features and 4 textural features, showed the highest AUC on the validation data set. Significant features and coefficients utilised in the models are manifested in Table S1.

Figure 2 and *Table 3* conclude the performance of the radiomic model with the SVM and LR methods. In the training and test dataset, the model based on SVM and LR methods demonstrated the highest performance compared with conventional imaging methods. AUCs of both models reached 0.93 (0.924–0.953) (SVM) and 0.93 (0.921–0.953) (LR) in the test dataset. At the high-sensitivity point, the SVM and LR model revealed diagnostic performance for diagnosis of calciphylaxis with the sensitivity, specificity, PPV and NPV of 0.89, 0.80, 0.80, 0.89 and 0.89, 0.85, 0.84, 0.90 respectively. At the high-specificity point, the SVM and LR model showed diagnostic performance for diagnosis of calciphylaxis with the sensitivity, specificity, PPV and NPV of 0.78, 0.90, 0.88, 0.82 and 0.78, 1.0, 1.0, 0.83 respectively.

In a subset of the test dataset, where patients had plain radiograph and bone scintigraphy, LR performed the highest AUC, followed by the SVM model (*Table 4*). Radiomics models illustrated higher AUCs than plain radiograph and bone scintigraphy (Delong test, P<0.05, Table S2). Bone scintigraphy also displayed a high specificity in the diagnosis of calciphylaxis.

Results of verification studies

As shown in *Figure 3*, in study I and III, the models on SVM and LR cannot classify (I) suspected lesions and L3 subcutaneous tissue in patients with suspected calciphylaxis and (II) L3 subcutaneous tissue in patients with confirmed calciphylaxis and that in patients with suspected calciphylaxis according to low AUCs (0.543–0.681). Despite this, in study II, the model with AUCs of 0.84 and 0.81 (SVM and LR respectively) performed better in the classification of skin lesions and L3 subcutaneous tissue in patients with calciphylaxis (*Figure 3*).

Table 1 Characteristics of patients

Characteristic	Training cohort			Test cohort		
	Calciphylaxis (+)	Calciphylaxis (−)	P value	Calciphylaxis (+)	Calciphylaxis (−)	P value
Patients, n	19	41		8	12	
Age, mean (SD), years	49.16 (13.45)	63.20 (15.21)	0.001	66.88 (13.22)	59.83 (12.64)	0.30
Sex, No. [%]	19 [100]	41 [100]	0.27	8 [100]	12 [100]	0.62
Male	13 [68]	20 [49]		7 [88]	9 [75]	
Female	6 [32]	21 [51]		1 [12]	3 [25]	
BMI, mean [SD], kg/m^{2a}	22.36 [4.10]	22.86 [3.62]	0.48	23.62 [3.41]	23.81 [50.02]	0.90
CKD level, No. [%]	19 [100]	41 [100]	0.30	8 [100]	12 [100]	−
4	0 [0]	4 [10]		0 [0]	0 [0]	
5	19 [100]	37 [90]		8 [100]	12 [100]	
Current cigarette smoker, No. [%]	1 [5]	5 [12]	0.65	2 [25]	2 [17]	>0.99
Alcohol abuse, No. [%]	0 [0]	0 [0]	−	0 [0]	0 [0]	−
Coronary artery disease, No. [%]	1 [5]	8 [20]	0.25	1 [13]	2 [17]	>0.99
Diabetes, No. [%]	4 [21]	21 [51]	0.03	4 [50]	5 [42]	>0.99
Diabetes mellitus type 1, No. [%]	1 [5]	1 [2]		0 [0]	0 [0]	
Diabetes mellitus type 2, No. [%]	3 [16]	20 [49]		4 [50]	5 [42]	
Hepatobiliary disease, No. [%]	4 [21]	4 [10]	0.25	3 [38]	1 [8]	0.26
Hypertension, No. [%]	15 [79]	37 [90]	0.25	7 [88]	11 [92]	>0.99
Hyperparathyroidism, No. [%]	7 [367]	4 [10]	0.03	3 [38]	3 [25]	0.64

[a]3 patients in training cohort with no available BMI data, and 1 patient in test cohort with no available BMI data. BMI, body mass index; CKD, chronic kidney disease; SD, standard deviation.

Table 2 Location of skin lesions and CT scan of calciphylaxis and suspected calciphylaxis patients

Patients	Location of lesions	Site of CT
Calciphylaxis patients		
1	Bilateral ankle	Lower extremities
2	Lower extremities	Lower extremities
3	Bilateral hands, Lower extremities, back	lower and upper extremities
4	Lower extremities	Chest, Abdomen, Lower extremities
5	Lower extremities	Chest, Abdomen, Lower extremities
6	Bilateral hands, Lower extremities	Abdomen, Lower extremities
7	Lower extremities	Chest, Abdomen, Lower extremities
8	Lower extremities	Lower extremities
9	Lower extremities	Chest, Lower extremities
10	Lower extremities, right foot	Chest, Abdomen, Lower extremities
11	Bilateral feet	Chest, Abdomen, Lower extremities

Table 2 (*continued*)

Table 2 (*continued*)

| Patients	Location of lesions	Site of CT
12	Left crus	Lower extremities
13	Lower extremities	Lower extremities
14	Lower extremities	Lower extremities
15	Right ankle, right foot	Lower extremities
16	Bilateral upper thighs, penis	Abdomen, Lower extremities
17	Lower extremities	Chest, Lower extremities
18	Left crus	Chest, Abdomen, Lower extremities
19	Lower extremities	Lower extremities
20	Lower extremities, right hand	lower and upper extremities, Abdomen
21	Lower extremities	Lower extremities
22	Bilateral feet	Abdomen, Lower extremities
23	Back	Chest, Abdomen, Lower extremities
24	Lower extremities	none
25	Abdomen	none
26	Lower extremities	Lower extremities
27	Bilateral hands, feet	none
28	Viscera	none
29	Bilateral hips	none
30	Back	Abdomen
31	Back	Abdomen
32	Lower extremities	lower extremities
Suspected calciphylaxis patients		
1	Left foot	Abdomen
2	upper extremities	Abdomen
3	Abdomen, lower extremities	Lower extremities, Abdomen
4	Abdomen, lower extremities	Abdomen, Lower extremities
5	Abdomen, lower and upper extremities	Chest, Lower extremities
6	Upper extremities	Abdomen
7	Lower extremities	Lower extremities
8	Abdomen	Abdomen
9	upper thighs	Lower extremities
10	Lower extremities	Lower extremities
11	Lower extremities, back	Abdomen, Lower extremities
12	Abdomen, lower and upper extremities	Lower extremities
13	left hand	upper extremities
14	Bilateral feet	Lower extremities
15	Lower extremities	Lower extremities
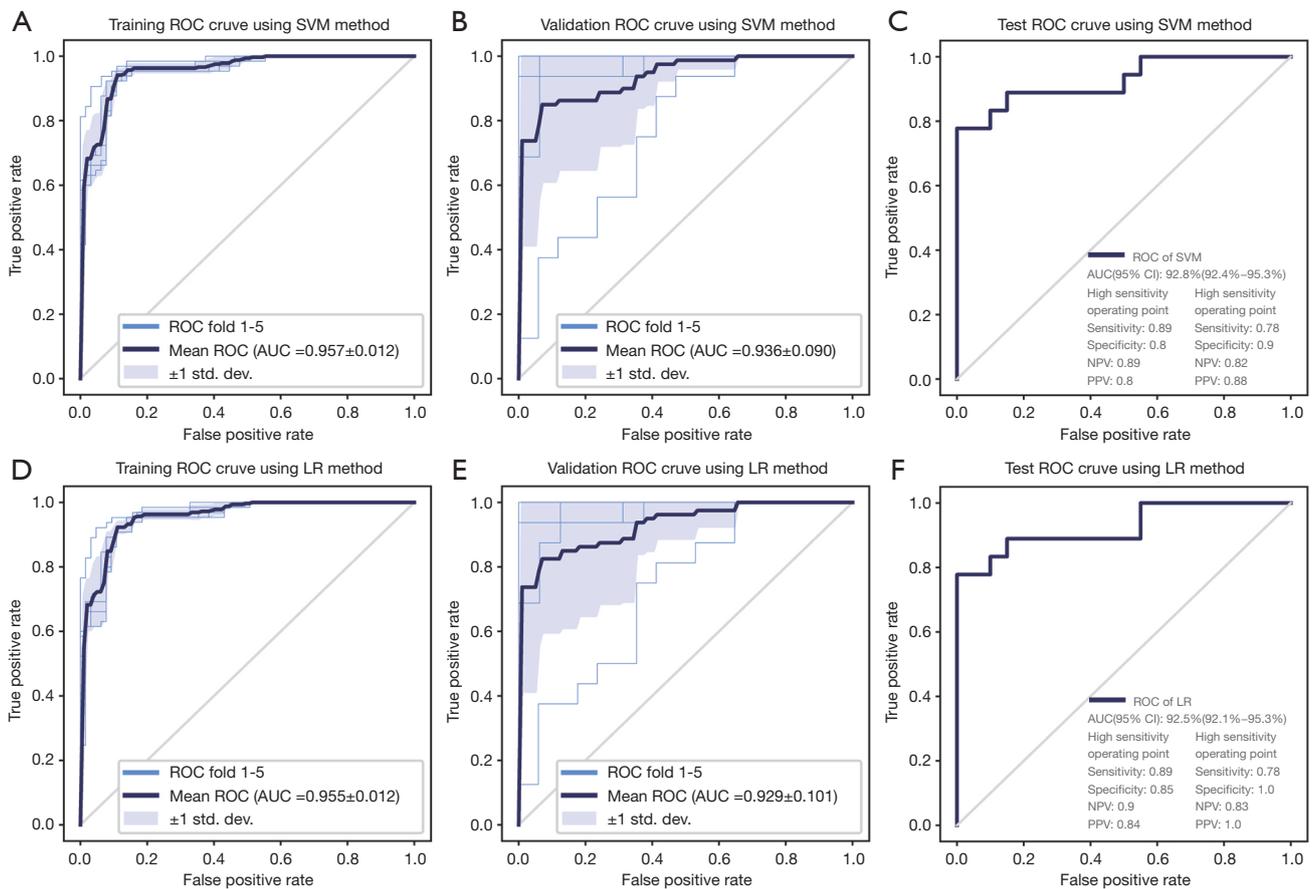
Figure 2 Predictive performance of models in training, inter-validation and test datasets. AUC, areas under the ROC curves; ROC, receiver operating characteristic; LR, logistic regression; SVM, support vector machine; PPV, positive predictive value; NPV, negative predictive value.

Table 3 Predictive performance of radiomic models[a]

	AUC (95% CI)	High sensitivity model				High specificity model			
		Sensitivity	Specificity	NPV	PPV	Sensitivity	Specificity	NPV	PPV
SVM	0.93 (0.924–0.953)	0.89	0.80	0.89	0.80	0.78	0.90	0.82	0.88
LR	0.93 (0.921–0.953)	0.89	0.85	0.90	0.84	0.78	1.0	0.83	1.0

[a]Total lesions: 38 (positive: 18/negative: 20). PPV, positive predictive value; NPV, negative predictive value; AUC, areas under the ROC curves; ROC, receiver operating characteristic; LR, logistic regression; SVM, support vector machine.

Discussion

In this retrospective study, it proposed the radiomics method and demonstrated the effectiveness of the noninvasive machine learning technique in diagnosing skin lesions in patients with calciphylaxis (*Figure 2*).

The sample comprised 27 histopathological confirmed calciphylaxis patients and 12 histopathological confirmed non-calciphylaxis patients with suspected skin lesions. Given the histopathological examination as the ground truth, the models in this research were confirmed to be stable and could be generalised in the diagnosis of skin lesions in calciphylaxis.

Calciphylaxis diagnosis is challenging. In the test

Table 4 Predictive performance compared with plain radiography and bone scintigraphy

	LR High sensitivity Model	LR High specificity Model	SVM High sensitivity Model	SVM High specificity Model	Plain radiograph (Presence of vascular calcification)	Bone scintigraphy
TP	13	12	13	12	10	7
TN	9	11	8	10	4	9
FN	1	2	1	2	4	7
FP	2	0	3	1	7	2
Sensitivity	0.93	0.86	0.93	0.86	0.71	0.50
Specificity	0.82	1	0.73	0.91	0.36	0.82
AUC	0.95		0.92		0.54	0.66
AUC 95% CI	0.86–1.0		0.80–1.0		0.31–0.71	0.42–0.88

LR, logistic regression; SVM, support vector machine; AUC, areas under the ROC curves; ROC, receiver operating characteristic; TP, true positive; TN, true negative; FN, false negative; FP, false positive.
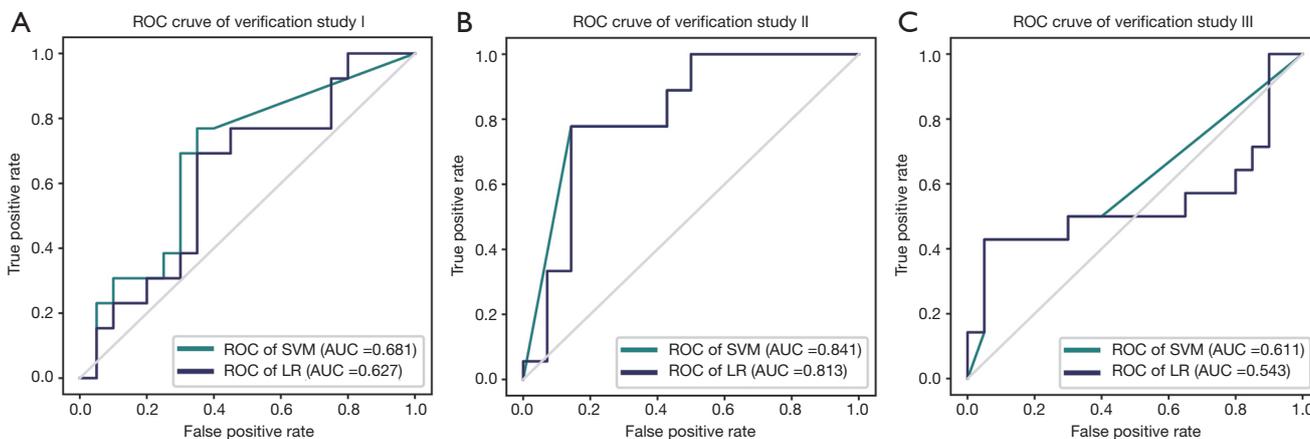
Figure 3 Results of verification studies. AUC, areas under the ROC curves; ROC, receiver operating characteristic.

dataset, radiomic models performed well for diagnosing calciphylaxis in CKD patients, which was better than conventional radiology methods such as plain radiograph and bone scintigraphy (*Table 3*), the performance of which was similar to that in previous studies (3,5). The exploration of diagnostic models has confirmed the possibility of a non-invasive diagnosis method that might provide clinicians with an alternative when histopathological examination is impossible and thereby reducing the incidence of complications due to invasive operations, especially at the skin lesions (2). However, bone scintigraphy also showed high specificity based on our dataset (0.82), while its sensitivity was 0.5. Specificity in this study is comparable to that in the research of Paul *et al.* (0.97) but the sensitivity

is much lower (0.89) (5). However, a more accurate noninvasive method can be provided for calciphylaxis diagnosis by combining radiomics methods on CT and bone scintigraphy.

Secondly, the radiomics and machine learning methods were adopted in this study, which are popular in disease diagnosis and prognosis prediction (9). In the models, 50% of the features included were first-order, while the rest were second-order. Nevertheless, they showed a potential to detect inflammation, fibrosis, and vascularity in adipose tissue, and made the model more robust by being less sensitive to an absolute value (17,18). Similarity in AUC, sensitivity and, specificity for SVM and LR methods demonstrated the robustness of the same radiomic features,

based on the prior studies' result that the classification method played the most dominant role in the variability of model (15).

In the verification studies, SVM and LR model could not classify suspected lesion and L3 subcutaneous tissue in suspected calciphylaxis patients well. Extracted features might not represent the tissue characteristic in different locations. As manifested in the results of Study II and Study III, our model revealed the possibility that in calciphylaxis patients, tissue in lesion would be distinctive compared to distant tissue like abdomen, and huge differences might not exist between calciphylaxis patients and other CKD patients at the location without skin lesion.

This research has several limitations. It was a retrospective study, and given the low morbidity of calciphylaxis, a small sample size of both patients and controls was enrolled. In the meantime, this research selected a special dataset of negative cases and lesions in training, which might give rise to selection bias. Secondly, this is a single-centre study, and model performance could be different in a large population and other centres. Future studies should explore and validate the noninvasive methods for diagnosis of calciphylaxis in more patients and centres including both imaging-based and serum-based methods.

To the best of our knowledge, this research is the first to develop a radiomics method in calciphylaxis diagnosis. CT radiomics features hidden within skin lesions were extracted and the radiomic model demonstrated preliminary feasibility as a noninvasive technique for calciphylaxis diagnosis in patients with CKD when invasive procedures are not available.

Acknowledgments

Footnote

Conflicts of Interest: All authors have completed the ICMJE uniform disclosure form (available at https://dx.doi.org/10.21037/qims-20-1211). The authors have no conflicts of interest to declare.

Ethical Statement: The authors are accountable for all aspects of the work in ensuring that questions related to the accuracy or integrity of any part of the work are appropriately investigated and resolved. This retrospective, cohort study was conducted in accordance with the Declaration of Helsinki (as revised in 2013) and was approved by the local institutional ethics review board. Additionally, the need for written informed consent from the participants was waived.

Open Access Statement: This is an Open Access article distributed in accordance with the Creative Commons Attribution-NonCommercial-NoDerivs 4.0 International License (CC BY-NC-ND 4.0), which permits the non-commercial replication and distribution of the article with the strict proviso that no changes or edits are made and the original work is properly cited (including links to both the formal publication through the relevant DOI and the license). See: https://creativecommons.org/licenses/by-nc-nd/4.0/.

References

1. Nigwekar SU, Thadhani R, Brandenburg VM. Calciphylaxis. N Engl J Med 2018;378:1704-14.

2. Nigwekar SU, Kroshinsky D, Nazarian RM, Goverman J, Malhotra R, Jackson VA, Kamdar MM, Steele DJR, Thadhani RI. Calciphylaxis: Risk Factors, Diagnosis, and Treatment. Am J Kidney Dis 2015;66:133-46.

3. Shmidt E, Murthy NS, Knudsen JM, Weenig RH, Jacobs MA, Starnes AM, Davis MD. Net-like pattern of calcification on plain soft-tissue radiographs in patients with calciphylaxis. J Am Acad Dermatol 2012;67:1296-301.

4. Halasz CL, Munger DP, Frimmer H, Dicorato M, Wainwright S. Calciphylaxis: Comparison of radiologic imaging and histopathology. J Am Acad Dermatol 2017;77:241-246.e3.

5. Paul S, Rabito CA, Vedak P, Nigwekar SU, Kroshinsky D. The Role of Bone Scintigraphy in the Diagnosis of Calciphylaxis. JAMA Dermatol 2017;153:101-3.

6. Colboc H, Moguelet P, Bazin D, Carvalho P, Dillies AS, Chaby G, Maillard H, Kottler D, Goujon E, Jurus C, Panaye M, Frochot V, Letavernier E, Daudon M, Lucas I, Weil R, Courville P, Monfort JB, Chasset F, Senet P; Groupe Angio-Dermatologie of the French Society of Dermatology. Localization, Morphologic Features, and Chemical Composition of Calciphylaxis-Related Skin Deposits in Patients With Calcific Uremic Arteriolopathy. JAMA Dermatol 2019;155:789-96.

7. Kramann R, Brandenburg VM, Schurgers LJ, Ketteler M, Westphal S, Leisten I, Bovi M, Jahnen-Dechent W, Knüchel R, Floege J, Schneider RK. Novel insights into

osteogenesis and matrix remodelling associated with calcific uraemic arteriolopathy. Nephrol Dial Transplant 2013;28:856-68.

8. Antonopoulos AS, Sanna F, Sabharwal N, Thomas S, Oikonomou EK, Herdman L, et al. Detecting human coronary inflammation by imaging perivascular fat. Sci Transl Med 2017;9:eaal2658.

9. Gillies RJ, Kinahan PE, Hricak H. Radiomics: Images Are More than Pictures, They Are Data. Radiology 2016;278:563-77.

10. Lambin P, Leijenaar RTH, Deist TM, Peerlings J, de Jong EEC, van Timmeren J, Sanduleanu S, Larue RTHM, Even AJG, Jochems A, van Wijk Y, Woodruff H, van Soest J, Lustberg T, Roelofs E, van Elmpt W, Dekker A, Mottaghy FM, Wildberger JE, Walsh S. Radiomics: the bridge between medical imaging and personalized medicine. Nat Rev Clin Oncol 2017;14:749-62.

11. McCarthy JT, El-Azhary RA, Patzelt MT, Weaver AL, Albright RC, Bridges AD, Claus PL, Davis MD, Dillon JJ, El-Zoghby ZM, Hickson LJ, Kumar R, McBane RD, McCarthy-Fruin KA, McEvoy MT, Pittelkow MR, Wetter DA, Williams AW. Survival, Risk Factors, and Effect of Treatment in 101 Patients With Calciphylaxis. Mayo Clin Proc 2016;91:1384-94.

12. Liu Y, Zhang X, Xie X, Yang X, Liu H, Tang R, Liu B. Risk factors for calciphylaxis in Chinese hemodialysis patients: a matched case-control study. Ren Fail 2021;43:406-16.

13. Di J, Liu Y, Wang D, Yang M. A Case of Early Calciphylaxis Diagnosed by Bone Scan. Case Rep Med 2020;2020:9526836.

14. van Griethuysen JJM, Fedorov A, Parmar C, Hosny A, Aucoin N, Narayan V, Beets-Tan RGH, Fillion-Robin JC, Pieper S, Aerts HJWL. Computational Radiomics System to Decode the Radiographic Phenotype. Cancer Res 2017;77:e104-7.

15. Parmar C, Grossmann P, Bussink J, Lambin P, Aerts HJWL. Machine Learning methods for Quantitative Radiomic Biomarkers. Sci Rep 2015;5:13087.

16. Chilamkurthy S, Ghosh R, Tanamala S, Biviji M, Campeau NG, Venugopal VK, Mahajan V, Rao P, Warier P. Deep learning algorithms for detection of critical findings in head CT scans: a retrospective study. Lancet 2018;392:2388-96.

17. Oikonomou EK, Williams MC, Kotanidis CP, Desai MY, Marwan M, Antonopoulos AS, et al. A novel machine learning-derived radiotranscriptomic signature of perivascular fat improves cardiac risk prediction using coronary CT angiography. Eur Heart J 2019;40:3529-43.

18. Elshafeey N, Kotrotsou A, Hassan A, Elshafei N, Hassan I, Ahmed S, Abrol S, Agarwal A, El Salek K, Bergamaschi S, Acharya J, Moron FE, Law M, Fuller GN, Huse JT, Zinn PO, Colen RR. Multicenter study demonstrates radiomic features derived from magnetic resonance perfusion images identify pseudoprogression in glioblastoma. Nat Commun 2019;10:3170.

TRIPOD Checklist: Prediction Model Development and Validation

Section/Topic	Item		Checklist Item	Page
Title and abstract				
Title	1	D;V	Identify the study as developing and/or validating a multivariable prediction model, the target population, and the outcome to be predicted.	1
Abstract	2	D;V	Provide a summary of objectives, study design, setting, participants, sample size, predictors, outcome, statistical analysis, results, and conclusions.	3
Introduction				
Background and objectives	3a	D;V	Explain the medical context (including whether diagnostic or prognostic) and rationale for developing or validating the multivariable prediction model, including references to existing models.	5
	3b	D;V	Specify the objectives, including whether the study describes the development or validation of the model or both.	5
Methods				
Source of data	4a	D;V	Describe the study design or source of data (e.g., randomized trial, cohort, or registry data), separately for the development and validation data sets, if applicable.	6-7
	4b	D;V	Specify the key study dates, including start of accrual; end of accrual; and, if applicable, end of follow-up.	6-7
Participants	5a	D;V	Specify key elements of the study setting (e.g., primary care, secondary care, general population) including number and location of centres.	6-7
	5b	D;V	Describe eligibility criteria for participants.	6-7
	5c	D;V	Give details of treatments received, if relevant.	NA
Outcome	6a	D;V	Clearly define the outcome that is predicted by the prediction model, including how and when assessed.	6-8
	6b	D;V	Report any actions to blind assessment of the outcome to be predicted.	6-8
Predictors	7a	D;V	Clearly define all predictors used in developing or validating the multivariable prediction model, including how and when they were measured.	7-11
	7b	D;V	Report any actions to blind assessment of predictors for the outcome and other predictors.	7
Sample size	8	D;V	Explain how the study size was arrived at.	6-7 Supplementary method
Missing data	9	D;V	Describe how missing data were handled (e.g., complete-case analysis, single imputation, multiple imputation) with details of any imputation method.	NA
Statistical analysis methods	10a	D	Describe how predictors were handled in the analyses.	7-11
	10b	D	Specify type of model, all model-building procedures (including any predictor selection), and method for internal validation.	7-11
	10c	V	For validation, describe how the predictions were calculated.	7-11
	10d	D;V	Specify all measures used to assess model performance and, if relevant, to compare multiple models.	7-11
	10e	V	Describe any model updating (e.g., recalibration) arising from the validation, if done.	NA
Risk groups	11	D;V	Provide details on how risk groups were created, if done.	NA
Development vs. validation	12	V	For validation, identify any differences from the development data in setting, eligibility criteria, outcome, and predictors.	7-11

Section	Item		Checklist Item	Page
Results				
Participants	13a	D;V	Describe the flow of participants through the study, including the number of participants with and without the outcome and, if applicable, a summary of the follow-up time. A diagram may be helpful.	12 Supplementary method
	13b	D;V	Describe the characteristics of the participants (basic demographics, clinical features, available predictors), including the number of participants with missing data for predictors and outcome.	12 Table 1&2
	13c	V	For validation, show a comparison with the development data of the distribution of important variables (demographics, predictors and outcome).	Table 1
Model development	14a	D	Specify the number of participants and outcome events in each analysis.	12 Table 1 Figure1
	14b	D	If done, report the unadjusted association between each candidate predictor and outcome.	NA
Model specification	15a	D	Present the full prediction model to allow predictions for individuals (i.e., all regression coefficients, and model intercept or baseline survival at a given time point).	12-14 Supplementary Table
	15b	D	Explain how to the use the prediction model.	12-14
Model performance	16	D;V	Report performance measures (with CIs) for the prediction model.	12-14, Table 3&4 Figure 2&3
Model-updating	17	V	If done, report the results from any model updating (i.e., model specification, model performance).	NA
Discussion				
Limitations	18	D;V	Discuss any limitations of the study (such as nonrepresentative sample, few events per predictor, missing data).	16
Interpretation	19a	V	For validation, discuss the results with reference to performance in the development data, and any other validation data.	14-16
	19b	D;V	Give an overall interpretation of the results, considering objectives, limitations, results from similar studies, and other relevant evidence.	14-16
Implications	20	D;V	Discuss the potential clinical use of the model and implications for future research.	14-16
Other information				
Supplementary information	21	D;V	Provide information about the availability of supplementary resources, such as study protocol, Web calculator, and data sets.	Supplementary material
Funding	22	D;V	Give the source of funding and the role of the funders for the present study.	17

*Items relevant only to the development of a prediction model are denoted by D, items relating solely to a validation of a prediction model are denoted by V, and items relating to both are denoted D;V. We recommend using the TRIPOD Checklist in conjunction with the TRIPOD Explanation and Elaboration document.

Method

Diagnosis protocol of calciphylaxis

Calciphylaxis diagnosis protocol was based on "Criteria for Diagnosis of Calciphylaxis" described in McCarthy et al. (11). One patient with risk factors and clinical conditions would receive multidisciplinary discussion including nephrology, dermatology, radiology, and pathology departments with experienced doctors.

In this study, we retrospectively reviewed our institutional datasets for patients with initial diagnosis of calciphylaxis. If one finally diagnosed as calciphylaxis, we included as calciphylaxis patients. If one with possible calciphylaxis but finally ruled out, we included as suspected calciphylaxis patients. Viscera calciphylaxis was not included in analysis. Finally, 32 patients were diagnosed according to reported diagnosis protocol(calciphylaxis) (11), and 15 patients were identified as suspected calciphylaxis from October 1, 2017, to November 30, 2019.

In the next step, we searched CT scan data involving lesion location. For example, if one patient had ulceration in right leg, we would find lower extremities non-contrast CT images in Picture Archiving and Communication Systems. All CT scan followed routine CT scan protocols. All images and masks were resampled to form isotropic voxels of unit dimension with 1 voxel corresponding to 1 mm^3 to ensure comparability. By centering the image at the mean with a standard deviation and re-charting the histogram to conform to l ± 3r (l: the average gray level within the VOI; r: the gray-level standard deviation), image normalization was realized.

Sample size consideration

For training, we used 70% (19 patients with 40 lesions) randomly chosen calciphylaxis patients and all CKD-non-calciphylaxis patients (41 patients with 82 patches) to form training cohort. To balance the case-to-noncase ratio as 1:1, we used SMOTE method to up-sample the calciphylaxis cases, which is a re-sampling technique commonly used in datasets. We applied 5-fold cross-validation on training data set to prove model performance. Eight features were selected after PCC and Relief, which making an event-per-predictor ratio >20. Therefore, we believed that there was no big concern on the overfitting issue of our model at this sample size.

For test, we used method introduced by Shein-Chung Chow and colleagues (19).

$$N_{positive} = N_{negative} = 2\left(\sigma \frac{z_{\alpha/2} + z_\beta}{\mu_{positive} - \mu_{negative}}\right)^2$$

where, N is the sample size for the validation group. Desired two-sided significance level of α = 0.05 ($z_{\alpha/2}$=1.96) and power of 1-β = 95% (z_β=1.64).

LR model: The sample sizes in the training groups were $n_{positive}$= 82(SMOTE) and $n_{negative}$= 82, with means of $\mu_{positive}$=0.3927 and $\mu_{negative}$=0.6075 respectively, and with a standard deviation of σ=0.1369. The minimum number of validation samples:

$$N_{positive} = N_{negative} = 2\left(\sigma \frac{z_{\alpha/2} + z_\beta}{\mu_{positive} - \mu_{negative}}\right)^2 \approx 11$$

SVM model: The sample sizes in the training groups were $n_{positive}$= 82(SMOTE) and $n_{negative}$= 82, with means of $\mu_{positive}$=0.1688 and $\mu_{negative}$=0.8133 respectively, and with a standard deviation of σ=0.3948. The minimum number of validation samples:

$$N_{positive} = N_{negative} = 2\left(\sigma \frac{z_{\alpha/2} + z_\beta}{\mu_{positive} - \mu_{negative}}\right)^2 \approx 10$$

Test dataset in our study included 18 calciphylaxis-positive and 20 calciphylaxis-negative lesions, which exceeded the minimum required sample sizes.

References

19. Chow S, Shao J, Wang H. Sample size calculations in clinical research. 2nd Ed. Chapman &Hall//CRC Biostatistics Series 2008.

Table S1 Features and coefficients of models

Features	Coef in model (SVM)	Coef in model (LR)
wavelet-LLH_glszm_GrayLevelVariance	1.330	1.187
wavelet-LLH_glcm_Imc2	2.930	2.524
wavelet-HLH_firstorder_Skewness	0.703	0.578
wavelet-HHH_glszm_LargeAreaLowGrayLevelEmphasis	0.594	0.316
original_firstorder_Kurtosis	-0.300	0.148
wavelet-LLL_firstorder_90Percentile	1.982	1.485
wavelet-LHH_firstorder_Median	3.460	2.168
wavelet-LLH_glcm_Imc1	−4.422	−3.164

Coef, coefficients.

Table S2 Results of Delong tests

ROC 1	ROC 2	p-value
LR	Bone scintigraphy	<0.01
LR	Plain radiograph	<0.01
SVM	Bone scintigraphy	0.02
SVM	Plain radiograph	<0.01

LR, Logistic Regression; SVM, Support Vector Machine; AUC, Areas under the ROC curves; ROC, Receiver operating characteristic.